Modelling Isolated Propeller Performance at High Angles of Attack

Sparsh Chadha[1], Jangho Park[2], Arun Subramanion[3]
PLANA, Gyeonggi-do, Yongin-Si, 16976, South Korea

The performance prediction of propellers in high angle of attack flows has become highly important in recent years due to advancement in the designs of Urban Air Mobility and Regional Air Mobility solutions which offer Vertical Take-off and Landing capabilities along with conventional cruise flight with tilting prop-rotors. A new aerodynamic model has been developed to predict the global performance parameters for isolated propellers in high angle of attack flows. The model presented here builds on top of the XROTOR platform to generate large amount of performance data at low computational cost which can be very valuable in early stages of design and support the development of control, stability and maneuvering strategy during the transition phase of the flight plan. The new methodology is validated with the wind tunnel test results of the XV-15 tilt rotor platform as well as with the computational and wind tunnel data for in-house blade design at different advance ratios, blade pitch angles along with different angles of attack and/or nacelle angles.

I. Nomenclature

C_T	=	Propeller Thrust coefficient
C_P	=	Propeller Power Coefficient
C_Q	=	Propeller Torque Coefficient
FOM		
RPM	=	Angular velocity of the propeller blade in Rotations per minute
α	=	Angle of attack
β	=	Blade pitch angle
η		
Ψ	=	Blade rotation angle
θ	=	Nacelle Angle
V_{fw}	=	Forward flight speed. Incoming freestream velocity
V_{ax}	=	Axial component of the freestream velocity along the propeller rotation axis
V_{inp}	=	In plane component of the freestream velocity in the plane of rotation of the propeller
V_{tan}	=	Tangential component of the velocity along the tangential direction of blade rotation
V_{radial}	=	Radial component of the velocity along the blade radial direction

II. Introduction

In recent years, there has been an increasing trend in the development of Urban Air Mobility and Regional Air Mobility solutions to solve traffic problems and reduce commuter time. Most solutions offer aircraft with Vertical Take-off and Landing (VTOL) and transition to cruise flight capabilities to allow for long range and high payload which is similar to a tilt-rotor configuration. As opposed to "Lift plus Cruise" configuration, in the conventional tilt-rotor configuration, the same propellers which provide lift during take-off and landing, also provide forward thrust during cruise flight. As a result, during the accelerating transition flight from hover mode to cruise mode, the propellers

[1] Lead of Aerodynamics, Research and Development Centre, PLANA, and AIAA Member
[2] Aerodynamics System Integration Engineer, Research and Development Centre, PLANA, and AIAA Member
[3] Aerodynamics Engineer, Research and Development Centre, PLANA, and AIAA Member

see an incoming freestream starting at 90 degrees angle of attack at the beginning of transition to 0 degrees angle of attack in cruise mode. The opposite is true for decelerating transition flight during landing.

The propellers installed on a tilt-rotor type aircraft configuration possess an additional rotational degree of freedom primarily used in transition flight to change the aircraft mode from rotor thrust based lift to wing borne lift. When presented as a function of aircraft airspeed and the nacelle angle, this type of flight envelope is called the "conversion corridor" [ref]. In the preliminary design phase of such an aircraft, it is highly critical to develop this part of the flight envelope to understand the basic performance requirements of both the aircraft and the propellers. This corridor represents a safe transition and aircraft trimmable environment within the allowable performance constraints. The conversion corridor marks several limitations including wing stall, aircraft attitude limit, and cruise torque limit for the electric motor. Figure 1 shows a typical conversion corridor for the XV-15 Tilt-rotor aircraft.

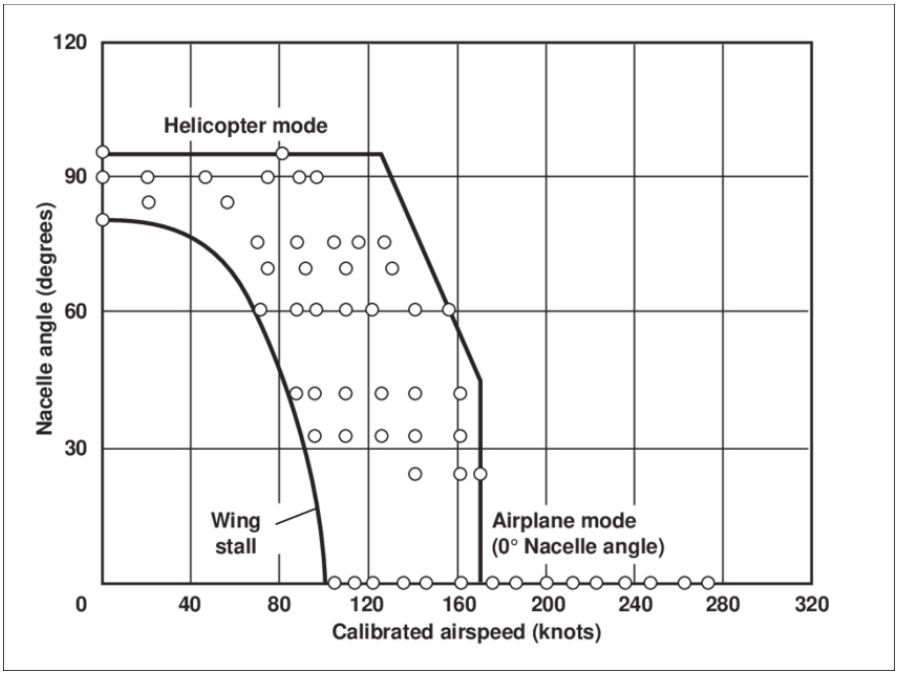

Figure 1: Conversion Corridor for XV-15 tilt-rotor aircraft (ref)

Due to the nature of the operating range of the propellers installed on tilt-rotor configuration aircraft, it becomes highly critical to predict the performance of propellers at high angles of attack flows as seen during the conversion corridor. Without over reliance on Computational Fluid Dynamics (CFD) methods, the current paper aims to predict the global performance parameters of the isolated propellers such as C_T, C_P and C_Q using low fidelity methods which can generate vast amounts of data at low computational cost. It is expected that the performance of the rotors will be a function of the angle of attack, RPM, blade pitch angle, flight speed and altitude all of which could change during the transition phase of the flight plan. The performance data is crucial for determining the optimum control, stability, and maneuvering strategy of the tilt-rotor aircraft in transition phase. In the preliminary design phase, over reliance on CFD methods or wind tunnel tests can increase the cost and lead time significantly in generation of such data. There are other tools and methods available to predict the performance of propellers/rotors at high angles of attack. One of them is CAMRAD II. However, ~~the program is~~open-source solutions to such expensive software are not ~~freely~~ available~~ and can be considered very expensive.~~. Hence,~~ in this paper, the author presents~~ a low fidelity aerodynamic model validated with high-fidelity methods which can predict the rotor performance and data points required in the early stages of design to prepare a safe transition map within the constraints of the conversion corridor~~.~~ has been presented in this work. The ~~set of~~ data set obtained through this method can also be used to build simulation models on ~~Flight Simulation~~flight simulation software that can be used for pilot training purposes.

Although there is an increasing list of organizations targeting entry into UAM and RAM market and with aircraft configurations ~~like a~~similar to tilt-rotor concept, there is very little public data available to validate the performance of propellers in the transition flight **[ref].** Many have used empirical methods to prepare aerodynamic models for predicting propeller performance. However, the experimental data available is mostly suited to specific set of propeller

blade designs and for specific operating conditions pertaining to ~~the use~~particular cases. The authors ~~in this method want to~~ present a generic methodology which can be applied to various propeller designs and different operating conditions pertaining to certain physics-based assumptions. Of course, there are many loads acting on the propeller operating in the conversion corridor. However, the scope of this paper is limited to predicting only the basic aerodynamic coefficients as mentioned earlier.

III. PLANA Aircraft and Blade specifications

PLANA is developing an aircraft for Advanced Air Mobility (AAM) market based on hybrid engine architecture. The aircraft would be capable of vertical take-off and landing through thrust borne flight and transition to highly efficient wing borne flight for cruise. The aircraft has a targeted Maximum Take off Weight (MTOW) of 7000 lbs and maximum range of 500 Kms at cruise speed of 300 Kmph. Figure 2 shows the configuration of PLANA's Full Scale Aircraft termed as CP-01. During take-off and landing, the thrust will be provided by 6 propellers with 5 blades each. With a combination of head and nacelle tilt, the propellers and nacelle transition to zero degrees nacelle angle from 90 degrees nacelle angle to support cruise borne flight.

Figure 2: Schematic illustration of PLANA's hybrid e-VTOL aircraft configuration

In order to validate the design process and feasibility, PLANA is developing a Proof of Concept (PoC) aircraft which is 1:5 scale of the Full-Scale aircraft. The scaled down aircraft is called as Mini Scale Demonstrator (MSD) nicknamed "Eclipse". Eclipse is targeted to have 6 propellers and features a canard configuration. Using multi-point design optimization, the Eclipse propeller blades were designed to operate and support VTOL flight as well as cruise flight efficiently. One of the key differences between the Full-scale propeller and Eclipse propeller is the number of blades (3 for MSD and 5 for Full-scale). The important geometric parameters for the Eclipse propeller blades are shown below in Table 1. Figure 3 and Figure 4 show the chord and blade pitch angle distribution along the blade span.

Table 1: PLANA's PoCs Blade specifications

Blade Diameter	0.8 m
Hub Diameter	0.06 m
RPM Range	2500 - 3000
Blade pitch angle range @ 60% span	0 to 40 deg
Number of Blades	3
Maximum Thrust	150 N
Nominal Thrust	76 N
Airfoil Section at 0.25R	E591
Airfoil Section at 0.75R	S7012

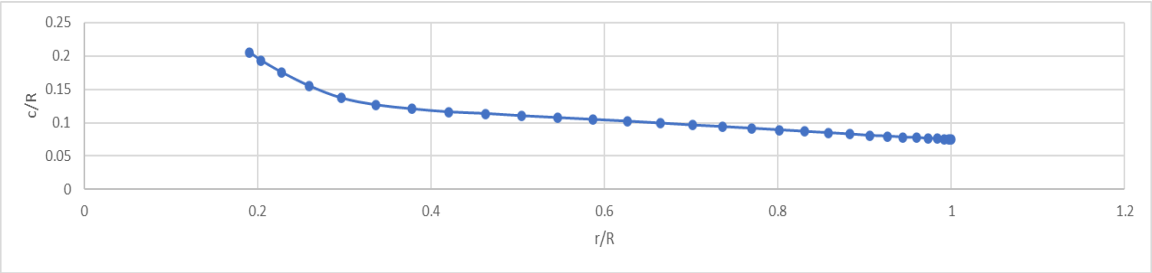

Figure 3: PLANA PoC's Blade Chord Distribution

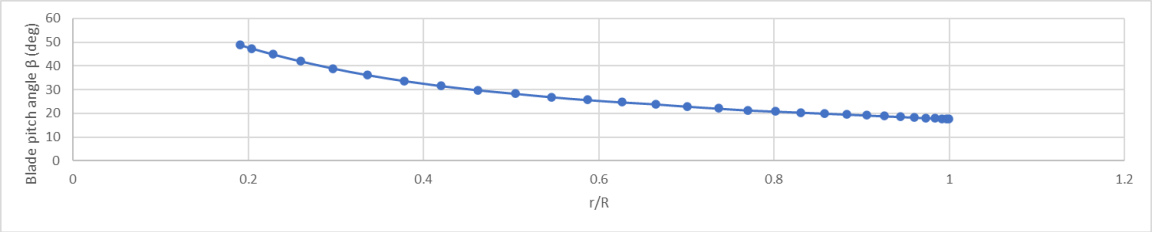

Figure 4: PLANA PoC's Blade Pitch Angle Distribution

IV. Methodology

The aerodynamic model presented here is built on top of XROTOR[1] platform which is an interactive program for the design and analysis of ducted and free-tip propellers and windmills. It is an open-source software released under GNU General Public License by creators Mark Drela and Hal Youngren. XROTOR is a useful tool in predicting propeller performance at zero-degree angle of attack and at low advance ratios. The authors exploit the key advantage of XROTOR for its ability to predict the performance of a propeller in incoming slipstream effects which can change radially along the blade. Hence, the user can define the incoming slipstream with an additional axial and tangential component. Ideally, this ability of the software is useful for the design and analysis of co-axial propellers as suggested by the creator of the tool in design notes. However, the novelty of the current methodology lies in the creative way one can use this ability of the software, validate the results with high order methods and Wind Tunnel tests as well as presents it in a simple to use manner for the UAM and RAM community.

In a mathematical sense, the methodology is as follows. The propeller axis of rotation is assumed to pass through the nacelle center line to be oriented with the incoming freestream velocity V∞ at θ degrees as shown in Figure ~~1~~4. At high angles of attack, the incoming flow towards the propeller can be broken down into an axial component (V_{ax}) and an in-plane component (V_{inp}). During one full rotation of the blade, the axial component as seen by the blade remains constant. However, the in-plane component as seen by the blade changes depending on the rotation angle as shown in Figure 2. Depending on the rotation angle, the in-plane component can be broken down further into a radial component and a tangential component to the blade. During the analysis, the input axial and tangential components are specified as inputs to the XROTOR platform. XROTOR is then run for complete range of blade rotation angle (Ψ) from 0 to 360 deg. Depending on the number of blades, the data for thrust, torque and power ~~is~~needs to be post processed which is a challenge. Of course, the data of relevance in the design purpose are the mean values in one rotation, however for validation purposes, the thrust, power and moment coefficients will be compared for every blade angle. For the scope of this study, the effect of radial component is ignored.

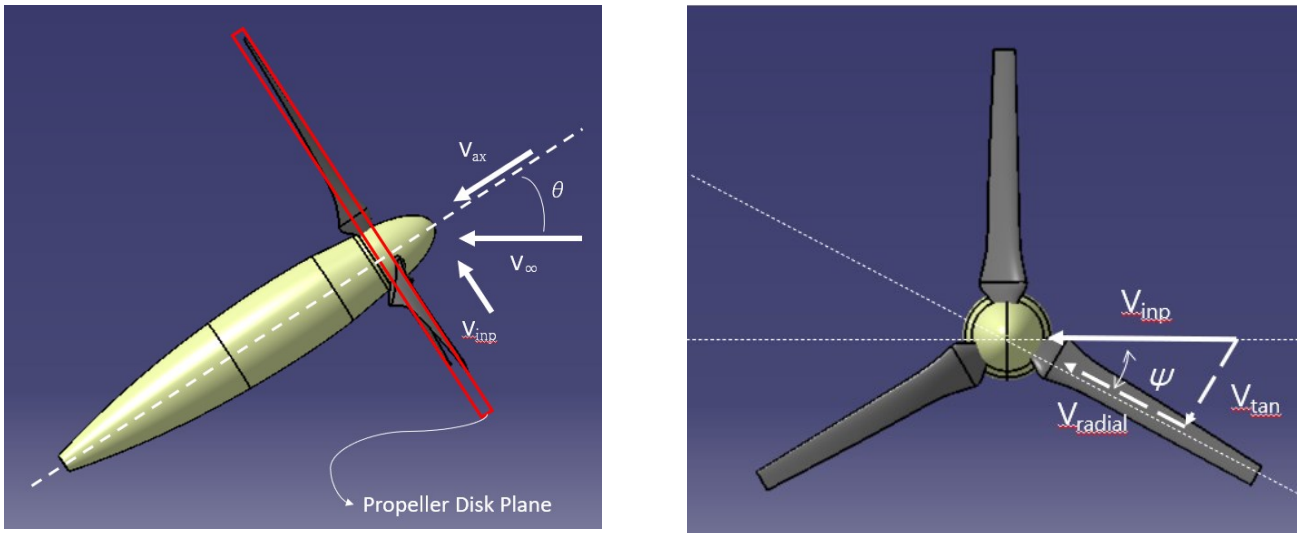

Figure 5: The forward flight speed (V_{fw}) is broken down into axial (V_{ax}) and in-plane (V_{inp}) component as seen by the propeller depending on the nacelle angle/ angle of attack (θ)

Figure 6: The V_{inp} is broken down further into tangential (V_{tan}) and radial (V_{radial}) component depending on the blade rotation angle (Ψ)

In terms of mathematical equations, the description of axial and in-plane velocity breakdowns is given below,

$$V_{ax} = V_\infty \times \cos\theta$$
$$V_{inp} = V_\infty \times \sin\theta$$

The in-plane velocity is further broken into tangential and radial components as follows

$$V_{tan} = V_{inp} \times \cos\Psi$$
$$V_{rad} = V_{inp} \times \sin\Psi$$

V_{ax} and V_{tan} are the inputs to the XROTOR program in order to define the incoming freestream velocity distribution along the blade span.

Following Figure 3, represents the block diagram for the methodology in a descriptive way.

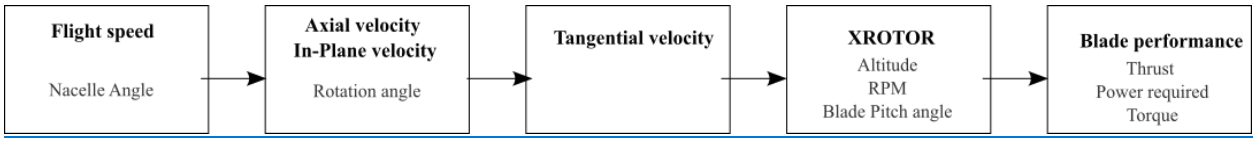

Figure 7: Figurative Summary of the described methodology. Parameters that are influential are shown in grey.

For a 3 bladed propeller, the staring position of each blade matters since that defines the blade rotation angle Ψ. A MATLAB program is written which calculates the V_{ax} and V_{tan} as inputs to the XROTOR program based on the user defined operating conditions including V_{inf}, RPM, Altitude, Blade pitch angle and Nacelle angle. This program also acts as a wrapper script and XROTOR is run through MATLAB in batch mode to generate the results quickly.

V. XROTOR Pre and Post Processing

In order to perform a propeller analysis in XROTOR, a comprehensive and detailed description of the propeller geometry and operating conditions is required. The blade geometry specifications include the chord and pitch distribution along the blade span, blade tip and hub radius and number of blades. The specifications of the operating conditions include the freestream velocity, advance ratio, *RPM*, and the ambient conditions such as altitude, speed of

sound, density, and dynamic viscosity. In addition to these, XROTOR requires two-dimensional airfoil aerodynamic data for various angles of attack and Reynolds number along the blade sections.

A. Pre-processing

For this study, the airfoil two-dimensional data was generated using XFOIL **[ref].** XFOIL is an interactive program for the design and analysis of subsonic isolated airfoils. The software has the same creators as XROTOR and is released under the GNU General Public License. It has various menu driven functions, the most important of which for the current study is the feature to analyze subsonic airfoils for different Reynolds numbers, angle of attack with forced and free transitions with viscous boundary layer. For PLANA's MSD propeller, the tip Mach number for all operating conditions is less than 0.4. Hence no compressibility corrections were applied to the aerodynamic data. While generating the two-dimensional aerodynamic data from XFOIL, forced transition at the airfoil leading edge was set to generate a full turbulent boundary layer for two reasons. The airfoil sections on the fabricated propeller blade may not experience a natural laminar boundary layer due to surface roughness and highly turbulent nature of the flow field as seen by propeller blades. The second reason is that the CFD models used later in the computational study are only turbulent models and this removes the uncertainty during data comparison that may arise due to boundary layer effects.

A MATLAB wrapper script was prepared to run XFOIL in batch mode at different angles of attack and Reynolds number that the airfoil sections are expected to experience during their operations for 2 airfoil sections. The airfoil section at *0.25R* was created using E591 airfoil and the airfoil section at *0.75R* was created using S7012 airfoil. These airfoils were selected during the detailed design process of the PLANA MSD propeller and the optimization and selection method used is outside the scope of this paper. Even though the selected airfoils have publicly available wind tunnel aerodynamic data **[ref],** the current work focusses only on computational tools at this moment to predict the eventual performance at high angles of attack. One of the major reasons for this is that, in the future design of Full-scale propellers, custom airfoils will be designed for which experimental data may not be available. Hence current work validates this design and performance prediction process through the means of the MSD propeller. Using this script, the following aerodynamic data for the airfoil sections were obtained.

1. Zero Lift Angle of attack (Cl_0)
2. Linear Lift curve slope (Cl_α)
3. Lift curve slope in stall region
4. Maximum Lift coefficient (Cl_{max})
5. Minimum Lift coefficient (Cl_{min})
6. Lift increment to stall
7. Minimum drag coefficient (Cd_{min})
8. Lift coefficient at minimum drag coefficient ($Cl_{@}Cd_{min}$)
9. Induced drag slope (dCd/dCl^2)
10. Pitching moment coefficient at aerodynamic center (Cm_{ac})
11. Reynolds number scaling exponent (Re_{scale})

B. Post-processing

The data obtained from XROTOR include the calculated thrust, power, torque, and propulsive efficiency. All the obtained data is along the axis of rotation of the propeller. For a propeller installed on tilt-rotor type aircraft, the axial velocity will be different than the flight velocity during transition. Hence it is important here to define the non-dimensional coefficients obtained and later compared in the validation process. As the propeller transitions from 90 degrees nacelle angle in VTOL model to 0 degrees in cruise mode, it not only produces axial force or thrust but also experiences side force, normal force, pitching moment, and yaw moment due to non-symmetric disk loading. The aerodynamic model proposed in this study can only predict the axial thrust and shaft torque and other forces and moments even though obtained from CFD and Wind Tunnel tests, will not be discussed. It is planned to improve the capability of the current model to be able to predict the remaining loads on the propeller and the motor shaft to form a complete Rotor dynamics model. Hence, for validation of the current model, the following quantities and their definition are used for data obtained from CFD and Wind Tunnel as well.

1. Propeller Advance Ratio

$$J = \frac{V_{inf}}{nD}$$

2. Thrust Coefficient

$$C_T = \frac{T}{\rho n^2 D^4}$$

3. Power Coefficient

$$C_P = \frac{P}{\rho n^3 D^5}$$

4. Torque Coefficient

$$C_P = \frac{C_P}{2\pi}$$

5. Blade Figure of Merit for Static Conditions

$$FOM = \frac{C_T^{3/2}}{\sqrt{2}C_P}$$

6. Blade Propulsive Efficiency

$$\eta = \frac{C_T}{JC_P}$$

XROTOR is an extension of Blade Element Momentum theory by **[ref]** and is an iterative solver through Newtonian iterations. It is possible that the software may not provide a converged solution at all the desired operating points. A curve fitting exercise needs to be done in order to correctly fit the predicted data for all blade rotation angles in one rotation cycle. Since the propeller blade sees a different incoming flow for different blade rotation angle Ψ, the thrust and torque produced also change as a function of Ψ. It was observed that due to the nature of the mathematical model, their behavior is periodic as a function of blade rotation angle. Hence the coefficients obtained above will be shown for average thrust, torque and power over one blade revolution. The positive peak amplitude and the negative peak amplitude may not be displaced by the same amount from the mean and hence a simple sine or cosine function cannot be used to approximately fit the predicted data. Hence, a 2nd order Fourier series expansion model shown below is used to fit the predicted thrust and torque values.

$$F(t) = c_o + c_1 \cos t + c_2 \cos 2t + d_1 \sin t + d_2 \sin 2t$$

Figure 8 below shows two different operating points where the thrust as predicted by the XROTOR model for Ψ from 0 to 360 degrees is shown as the blue data points and the red curve is the 2nd order Fourier series that has been fitted to the data points. In Figure 8 (left), the XROTOR model converged for all the values of Ψ. However, on the right, the XROTOR model did not converge for values of Ψ between 50 to 120 degrees. Even though the model did not converge for some points, the Fourier series curve fitter accurately fits the data points. This is important while calculating the average thrust, torque and power of the blade in one revolution since some of the Ψ values are close to the peak and can significantly alter the mean values.

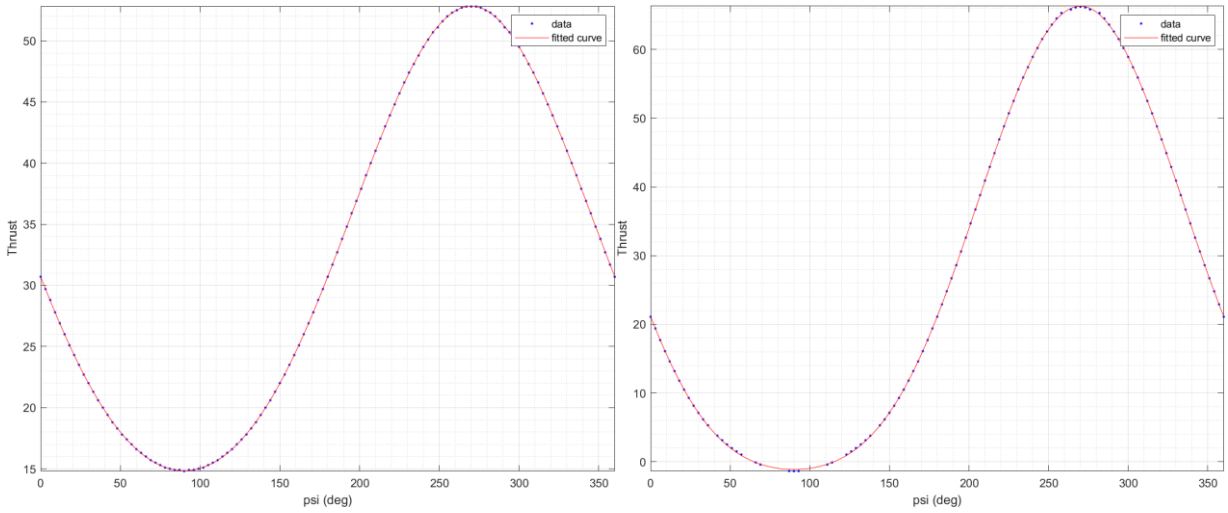

Figure 8: Evolution of the thrust based on the rotation angle of the blade from 0 to 360 degrees at two operating points.

Hence the finite data points obtained from the XROTOR model, converged or not, are fitted to a 2nd order Fourier series for axial Thrust and Torque values as shown below.

$$T(\Psi) = c_o + c_1 \cos\Psi + c_2 \cos 2\Psi + d_1 \sin\Psi + d_2 \sin 2\Psi$$

$$Q(\Psi) = a_o + a_1 \cos\Psi + a_2 \cos 2\Psi + b_1 \sin\Psi + b_2 \sin 2\Psi$$

$$P(\Psi) = Q(\Psi)\omega$$

The average thrust and torque values are obtained as below,

$$T_{avg} = \frac{\sum_{\Psi=0}^{\Psi=360} T(\Psi)}{\sum_{\Psi=0}^{\Psi=360} \Psi}$$

$$Q_{avg} = \frac{\sum_{\Psi=0}^{\Psi=360} Q(\Psi)}{\sum_{\Psi=0}^{\Psi=360} \Psi}$$

$$P_{avg} = \frac{\sum_{\Psi=0}^{\Psi=360} P(\Psi)}{\sum_{\Psi=0}^{\Psi=360} \Psi}$$

The above averaged values of Thrust, Torque and Power are used to calculate the propeller aerodynamic coefficients, FOM and efficiency.

VI. Computational and Experimental Setup

The novel method for propeller performance prediction proposed in this paper should be subjected to extensive validation and verification means. This is carried out using high fidelity Computational Fluid Dynamics (CFD) methods and wind tunnel testing. The following sections describe the basic setup.

A. Computational Method

The propeller geometry specified in section III is converted to a 3D CAD model using CATIA. The three-dimensional flow field around the propeller is solved using Siemens STARCCM+ with unsteady Reynolds Averaged Navier Stokes (RANS) simulation. Based on literature review **[ref],** a K-omega two equation turbulence model was used. The computational domain is cylindrical shape with semi spherical inlet and flat circular outlet. It extends 5 times the propeller diameter upstream and 10 times downstream of the propeller. The diameter of the cylindrical computational domain is 10 times the diameter of the propeller as shown in Figure 9.

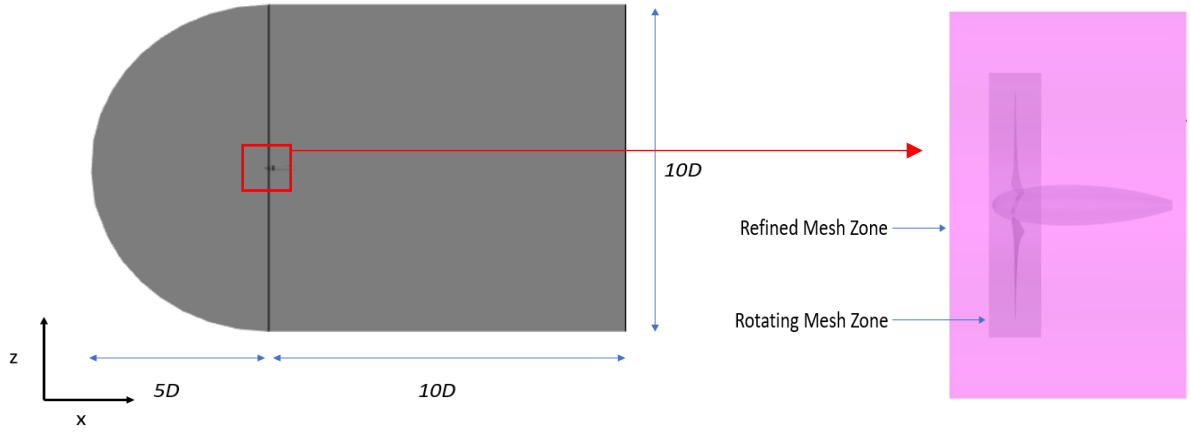

Figure 9

A high mesh density refined cylindrical domain was defined from 0.5 times the radius of the propeller in upstream and 2 times the radius in downstream direction to accurately capture the propwash of the propeller especially in the

wake as shown in Figure 9. A velocity inlet boundary condition was defined at the inlet which specified the incoming flow velocity, temperature, and pressure. This value is same as the V_{inf} in the XROTOR model. A pressure outlet boundary condition was defined at the outlet. A free-slip wall boundary condition was defined for the cylindrical sections since the authors observed convergence issues with freestream boundary condition.

Sliding mesh technique was used to simulate the blade rotation at specified *RPM*. In order to achieve this, a rotation zone was defined around the propeller blades including the head spinner part of the nacelle as shown in Figure 9. An interface was defined between the rotating zone and the steady zone to accurately use the sliding mesh technique. In order to simulate geometrical changes such as the nacelle angle and blade pitch angle, the whole geometry of the propeller plus nacelle was changed and re-meshed for the next configuration instead of changing the boundary conditions. To simulate different propeller advance ratios, the velocity specification at the inlet and the rotation rate for the rotation zone were changed. The simulation was assumed to be satisfactorily converged when the residuals of continuity and momentum reached values less than 10^-3 and the thrust and torque monitors reached a periodic steady state. After several trial runs, this was achieved within 10 blade rotations and hence all the simulations were run for that duration. The time step size for unsteady simulation was kept corresponding to 3 degrees of rotation angle. Hence the time step size was different for different *RPM*s.

A grid convergence study was conducted to arrive at a satisfactory mesh size to validate the CFD simulations. Four different meshes with coarse, medium, and fine settings along with hub refinement were generated and the value of thrust coefficient and torque coefficient were monitored. The different mesh sizes and their settings are listed below in Table 2. Figure 10 shows the quadrilateral surface mesh distribution on the propeller blades with increasing refinement from left to right. Figure 11 shows the additional refinement of mesh at the intersection point of the blade root with the nacelle.

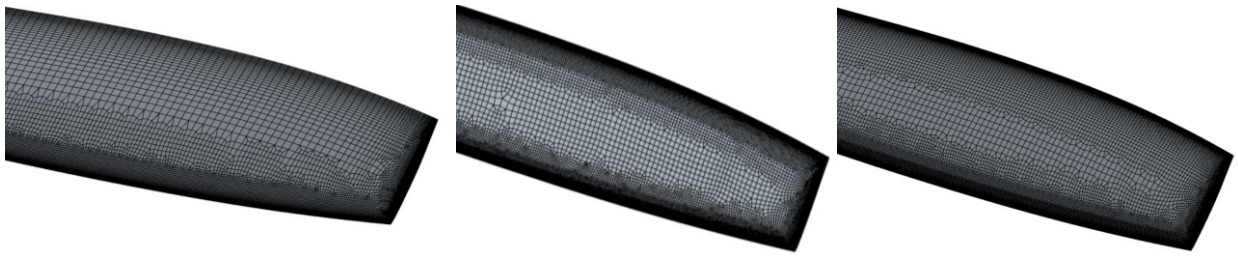

Figure 10: Quadrilateral Mesh distribution on the blade surface in increasing order of refinement from left to right. (0.8 to 1.0 *r/R* is shown)

Table 2

	Coarse 1	**Medium 1**	**Medium 2**	**Fine**
Mesh elements	12 million	18 million	20 million	40 million
mesh	No hub refinement	No hub refinement	Hub refinement	Hub refinement
Cores	360	360	360	720
Number of Prism Layers	5	8	8	10

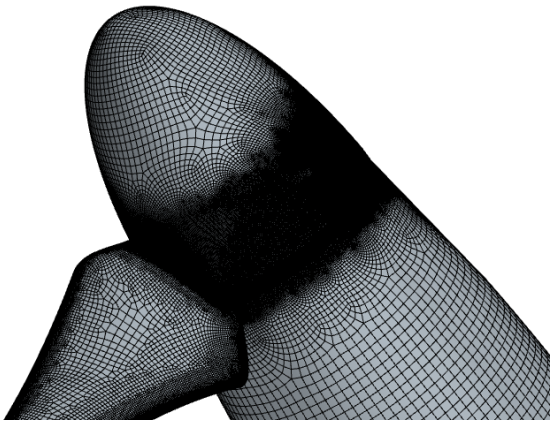

Figure 11: Refinement of mesh elements near the hub of the propeller blades

Figure 12: Velocity distribution of flow field around the propeller for coarse (left) and fine (right) mesh

With roughly four times the increase in mesh size from the coarsest mesh to the finest mesh, Figure 12 shows no qualitative changes in the flow features through the velocity distribution. Figure 13 shows that the values of C_T, C_P and C_Q do not change significantly (no change till 3rd decimal place) as the mesh size is increased from 12 million to 40 million. Additionally, the Grid Convergence Index (Richardson extrapolation technique by Roache**) [Roache P. (1997). Quantification of uncertainty in computational fluid dynamics. *Annual Review of Fluid Mechanics*, *29*(1), 123–160. doi: 10.1146/annurev.fluid.29.1.123]** showed that the medium mesh (20 million cells) deviated less than 1% from the Richardson extrapolation. Hence the 3rd mesh option with 20 million cells and hub refinement was chosen to conduct all the computational studies. The simulations were run on Amazon Web Service's (AWS) HPC cloud computing platform using 10 nodes (each node with 36 CPUs) to get the solution for each operating case and geometry in roughly 4 hours of computational time.

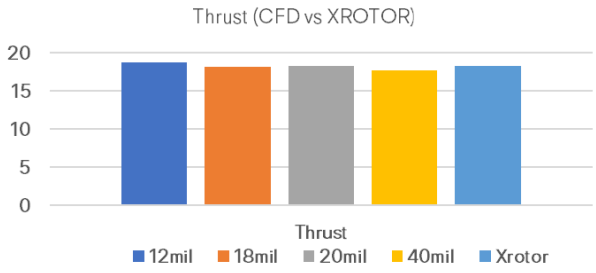

	12mil	18mil	20mil	40mil	Xrotor
Thrust	**18.64**	**18.05**	**18.18**	**17.61**	**18.2**
Moment	3.3	3.23	3.215	3.141	2.93
C_T	0.015	0.014	0.014	0.014	0.014
C_Q	0.003	0.003	0.003	0.003	0.003
C_P	0.020	0.020	0.020	0.019	0.018
Eta	0.736	0.728	0.736	0.730	0.809

Figure 13

B. Experimental Method

The verification of the CFD simulations and XROTOR software was done using wind tunnel testing. The designed propeller blade was fabricated in house using composite material and tested at the Republic of Korea Air Force Academy (ROKAF) Wind tunnel ref. Figure 14 shows the Eclipse blades manufactured in-house at PLANA's

facilities. The ROKAF low speed wind tunnel features a test section size of 3.6 m height and 5 m in width with maximum test section speed of 80 m/s. The personnel and the facility have experience with testing of various low speed UAVs, high speed military fighters and propeller blades. The cross-section of the test section was ample to avoid wall interreference effects with the propeller blades of the Eclipse aircraft which have a diameter of 0.8 m.

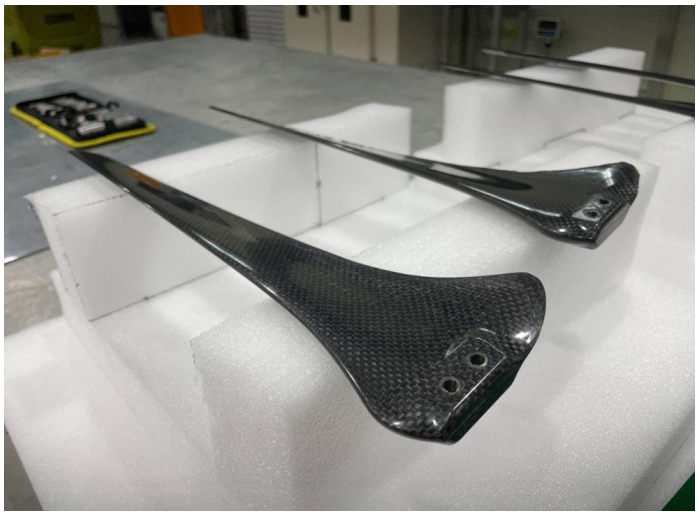

Figure 14

Figures 15 and 16 below show the installed assembly of the propeller, nacelle and the measurement sting at Nacelle angle of zero degrees and 90 degrees respectively. Even through PLANA's full-scale aircraft as shown in Figure 2 has a head tilt mechanism instead of nacelle tilt, wind tunnel tests were conducted for both head tilt and nacelle tilt. For purposes of this study, only nacelle tilt data is made available. The Blade pitch mechanism, ESC and the motor are installed inside the Nacelle assembly. For the purposes of this test, the KDE brushless motor with model number KDE8218XF-120 and KDE ESC with model number KDE-UAS125UVC-HE were used. The power supply cables for the motor, ESC and blade pitch mechanism were passed through the Nacelle and around the sting and connected to a High and Low voltage power supply located outside the test section to avoid interference effect.

Figure 15: Eclipse Propeller Model setup in the ROKAF Wind Tunnel at 0 degrees Nacelle angle (left) and 90 degrees Nacelle angle (right)

For verification purposes, wind tunnel tests were conducted for static runs (wind tunnel turned off) which simulates the hover condition in VTOL mode and runs with nacelle angle of zero degrees for different incoming velocities and propeller RPM which simulates the cruise condition. During both sets of runs, blade pitch angles were changed using PLANA's proprietary blade pitch-change mechanism. Figures 16 and 17 below show the comparison of XROTOR, CFD and Wind tunnel thrust and power coefficients for static and cruise conditions respectively. From the comparison, we can see that XROTOR over predicts the thrust for same required power as compared to both CFD and wind tunnel data. It is to be noted that the power vs thrust curve for CFD, and wind tunnel is aligned but the test points are not the same since they have different blade pitch angles. Due to limitations of the motor and blade-pitch mechanism, it was not possible to exactly meet the desired blade pitch angles. From Figures 16 and 17 we can see that the XROTOR values are very close to the high fidelity CFD and experimental values which establishes that the method for validation and testing is complete.

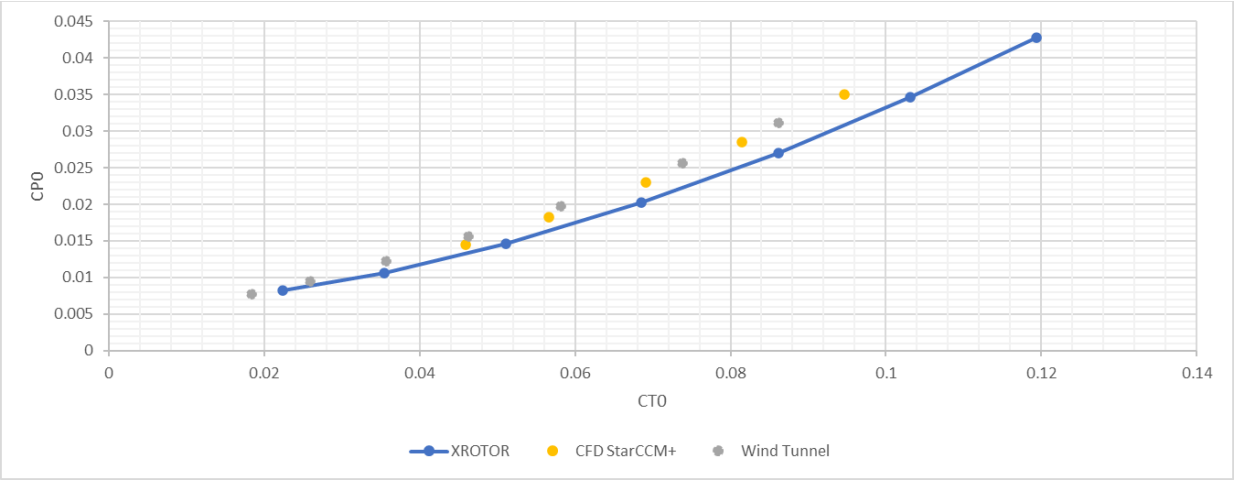

Figure 16: C_{T0} vs C_{P0} from XROTOR, CFD and Wind Tunnel for Eclipse Propeller blades at static conditions

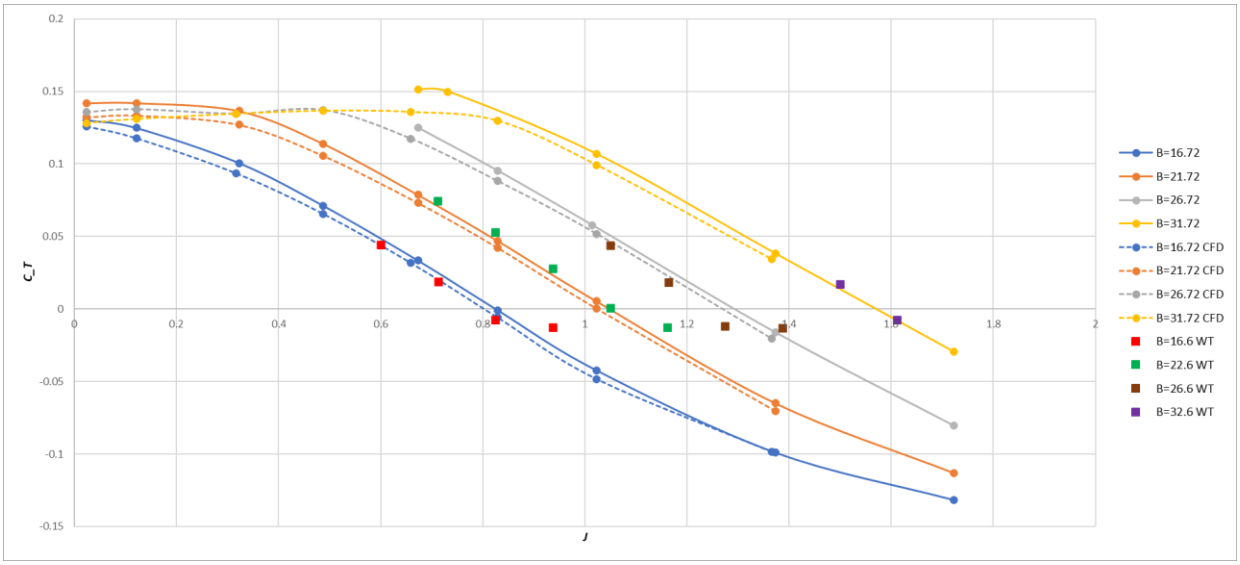

Figure 17: C_{T0} vs C_{P0} from XROTOR, CFD and Wind Tunnel for Eclipse Propeller blades at freestream conditions

VII. Results

The results of the method presented in this paper are validated and verified by the following means.

1. Experimental data of XV-15 tilt-rotor blade performed at NAFC (Closed Wind tunnel) and OARF (Open Air) wind tunnel and Flight test data [2,3,4]
2. CFD data from StarCCM+ u-RANS simulations for Eclipse propeller blades
3. Wind tunnel data from ROKAF for Eclipse propeller blades

A. Comparison with XV-15

The propeller blades of XV-15 Tilt rotor aircraft were tested at the NACF and OARF wind tunnels for different nacelle angles **ref**. It forms the key basis for the development of this model and a means for verification. The XV-15 tilt-rotor propeller geometric data is available in reference. Using this data, an XROTOR model of the propeller blades was developed as per the method described in section #. Ref also provides the performance predictions of the XV-15 propellers for static and cruise conditions. These data are used as means of validation of the XROTOR software first. Following figures shows the comparison

Data for XV-15 tilt-rotor blades at non-zero nacelle angles is then compared with XROTOR model predictions described in the current paper for different advance ratios. The following table shows the points which have been compared.

Table 3

	Values
Advance Ratio J	0.32
Nacelle Angle θ [deg]	15,30,60,75

Following set of figures shows the comparison

We can see that for low Nacelle angles at 15 and 30 degrees the XROTOR model values are very close to the wind tunnel data. At high nacelle angles of 60 and 75 degrees, the XROTOR model values are much closer to CAMRAD II data as compared to wind tunnel data. Overall, the trend of the power and thrust coefficients closely follow the data from Wind Tunnel and CAMRAD II values. It should be observed that the data from CAMRAD II also deviates from the wind tunnel data for high nacelle angles. This exercise forms a good basis of validation for the current model to be used for testing the performance prediction of the design of the PLANA's MSD aircraft blades.

B. Comparison with Computational Method

Table 4 lists the operating points that are used for comparison between CFD and XROTOR model for the Eclipse propeller. These set of points are some of the most important points for the conversion corridor flight envelope of Eclipse and hence are used as a baseline for comparison. It should be noted that at these operating points the blade does not stall.

Table 4

	Values
Advance Ratio J	0.3, 0.4
Nacelle Angle θ [deg]	45, 60, 75
Blade Pitch Angle β [deg] @ 60% r/R	5.2 to 17.2 in steps of 3 for J=0.3 and from 11.2 to 29.2 in steps of 3 for J=0.4

First, the points for Nacelle Angle of 75 degrees are compared. For an advanced ratio of 0.3 (V_inf=10 m/s and RPM = 2500), we can clearly see that the XROTOR model predictions are very close to the CFD values in **Figure** . The Blade stall is expected around CT of 0.12. As the thrust coefficient increases and gets closer to the stall point, we can see that the deviation between CFD and XROTOR model increases.

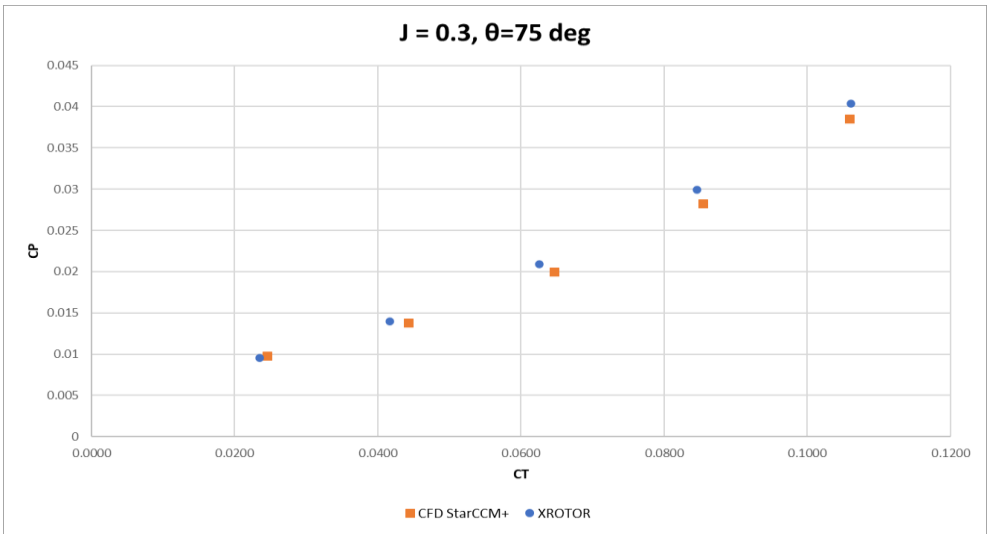

Figure 18

The next set of data points are for same nacelle angle but higher advance ratio of 0.4. As per the A/C design and the conversion corridor of Eclipse, it is not expected to experience this high advance ration for nacelle angle of 75 degrees. However, to test the limitations of CFD and of the model some additional blade pitch angles points were calculated. From the Figure, we can clearly see that the propeller experiences stall around C_T of 0.13 with a C_T max of 0.14 form the CFD data. The XROTOR model shows higher deviations from CFD values, and the deviation increases significantly close to stall. The XROTOR model shows blade stall but at a higher CT value of around 0.145. There could be several reasons for this behavior. Starting with the two-dimensional airfoil database used in XROTOR is obtained from XFOIL. Secondly, the flow during blade stall is highly separated three-dimensional flow. Since many three-dimensional effects are ignored in this mathematical model, it fails to predict the flow behavior and consequently the propeller performance close to stall. Another interesting thing to note is that even before blade stall, there is high deviation between the XROTOR and CFD values as compared to lower advance ratio data. One good thing is, however, the thrust coefficient values predicted by the XROTOR model are on the conservative side i.e., for some power coefficient the XROTOR model under predicts the thrust. Similar behavior was observed on comparison with the XV-15 results in section VII A. Since, the authors propose this tool for the conceptual or preliminary design phase of the aircraft, conservative values may be acceptable by some designers.

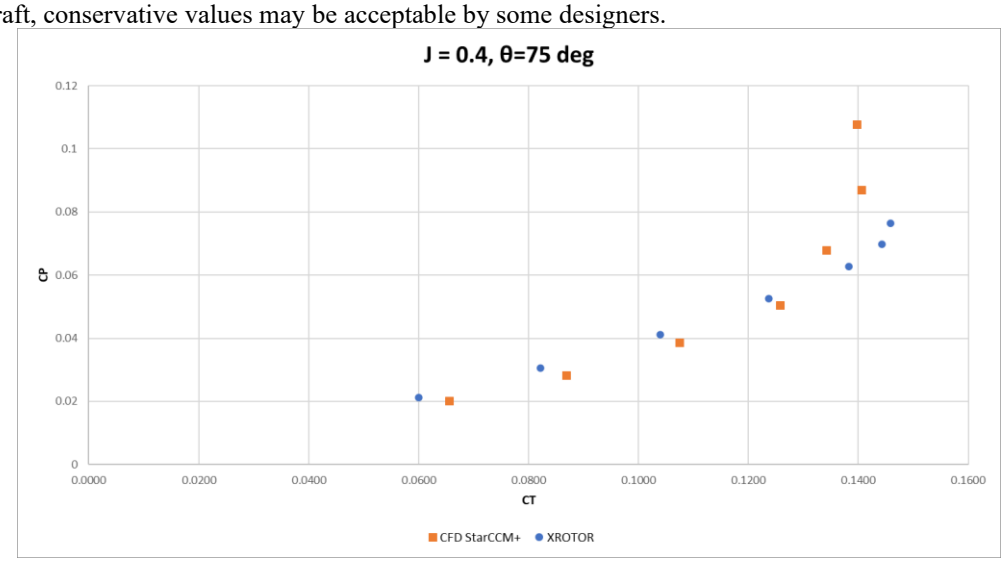

Figure 19

Figure and show the comparison of CT and CP at nacelle angle of 60 degrees and 45 degrees respectively and advance ratio of 0.3. Again, at lower advance ratio, the data points are closer to each other. However, it can be clearly seen that as the thrust coefficient increases, the deviation between XROTOR and CFD values also increases.

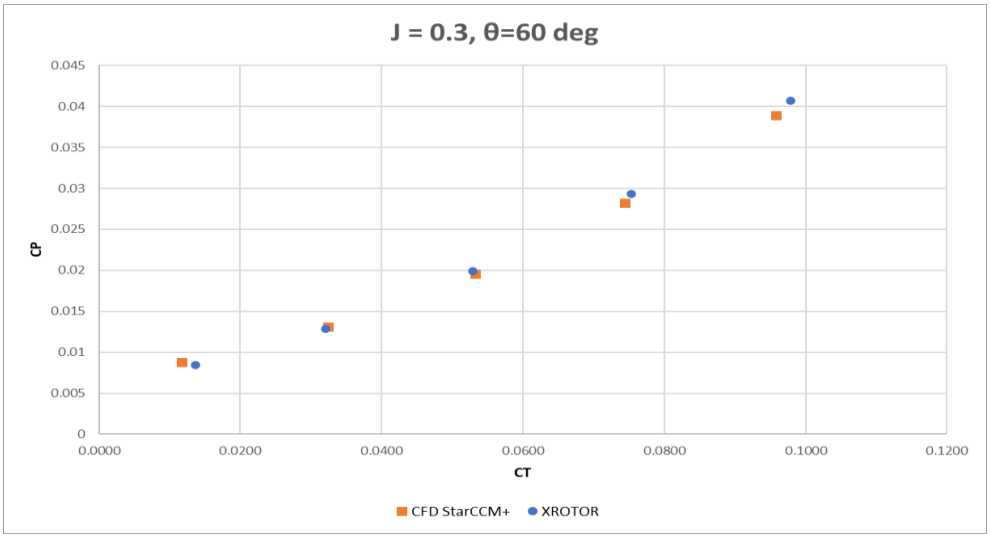

Figure 20

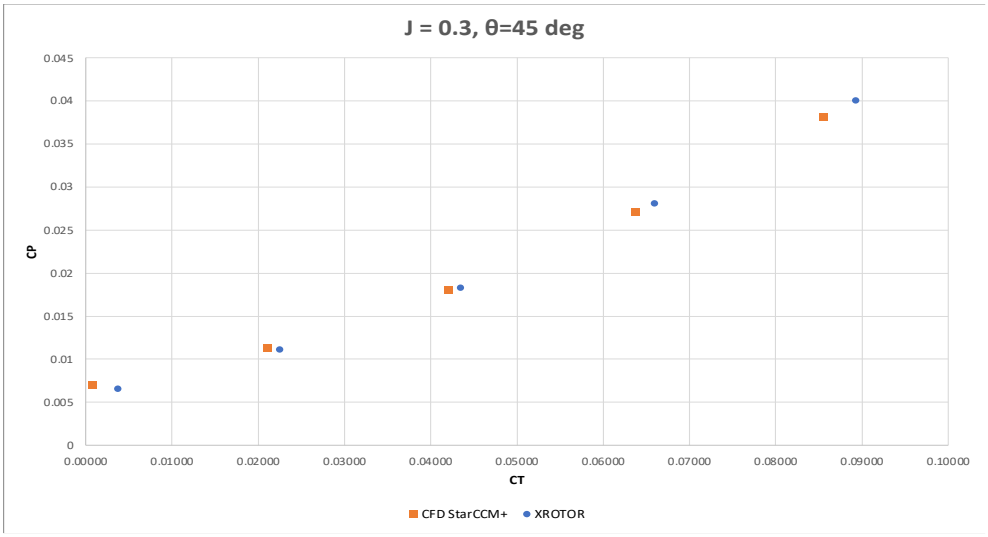

Figure 21

C. Comparison with Experimental Method

By applying a side slip angle, the wind tunnel model was tested for different Nacelle angles and advance ratio in the ROKAF wind tunnel as described in Section VI B. The blade pitch mechanism was not able to exactly match the CFD blade pitch angle test points. Also, the limitations of the motor peak torque, meant that the blade pitch angle point had to be carefully chose. Hence the test matrix for the wind tunnel model is different from the CFD model and is shown in table below.

	Values
Advance Ratio J	0.4, 0.6
Nacelle Angle θ [deg]	45, 60, 75
Blade Pitch Angle β [deg] @ 60% r/R	11.2 to 21.2 in steps of 3

VIII. Conclusions

This paper proposes a simple model to calculate isolated propeller performance coefficients at high angles of attack mostly experienced by the propeller blades during the transition flight of a tilt-rotor aircraft configuration. The authors use a freely available tool XROTOR and try to expand its capability to predict performance coefficients in a highly complex three-dimensional flow field. The predicted values show good agreement with CFD and experimental methods. The trends in thrust and power coefficient as predicted by the proposed model show a good co-relationship with high fidelity CFD simulations and experimental methods which are costly and time consuming. The model, however, does have limitations in the predictions few of which can be attributed to the inherent assumptions made during its development.

1. The XROTOR model fails to predict blade stall at different Nacelle angles. It is one of the most important limitations of the model and can be attributed to several factors. The XROTOR program itself fails to predict blade stall in static conditions. The two-dimensional database provided to XROTOR is generated from XFOIL which may not predict 2D airfoil stall accurately. Future work may involve preparing the two-dimensional database using experimental airfoil data.

2. As the advance ratio increases, the results from the XROTOR model deviate from CFD and wind tunnel values. One of the important assumptions made in the model development was to ignore the effect of spanwise flow. However, with increasing advance ratios, the incoming freestream velocity increases and its spanwise component increases as well. With higher spanwise flow velocities, the load distribution on the blade could start changing significantly which can lead to deviation in the predicted thrust and power coefficients from the model.

3. Due to asymmetric velocity distribution on the propeller plane, the propeller and motor shaft experiences other forces and moments such as side force, pitch moment and yaw moment. These forces and moments are not calculated by the current model. In the future, the authors plan to use the knowledge of velocity distribution along the propeller plane in one blade rotation to estimate these forces and moments to develop a complete Rotor Dynamics model that can be useful in the structural design of the tilting mechanism.

However, even with these limitations, if the current model is used appropriately and within its limitations, it can give propeller performance trends for high angles of attack. This preliminary data can be very useful in the design of the transition control logic and prepare the conversion corridor flight envelope of a tilt-rotor configuration during the initial stages of aircraft design. The transition phase of a tilt-rotor aircraft is one of the most difficult flight phases for the pilot to maneuverer. Data from the current model can be useful in setting up the flight simulator which can be used to train the pilots from the start. Hence, according to the authors this model can become a very useful tool in the initial design and performance analysis phase for aircraft configurations whose propellers experience high angle of attack flows. It expands on the capability of freely available XROTOR tool and becomes handy for start-ups and initial stage companies targeting to enter the AAM space with limited financial and extremely high time constraints.

Acknowledgements

The authors would like to express their gratitude to Republic of Korea Air Force academy and their personnel for supporting the wind tunnel activities mentioned in this paper. The authors would also like to acknowledge Amazon Web Services (AWS) for supporting the computational work on their HPC Cloud platform.

IX. Preliminary data

The preliminary results of the model described are presented here as compared with the XV-15 tilt-rotor wind tunnel data and data from CAMRAD II software [2,5]. Figure 4 and Figure 5 below show the prediction of Power vs thrust coefficient for advance ratio of 0.32 and nacelle angle of 30 and 15 degrees respectively.

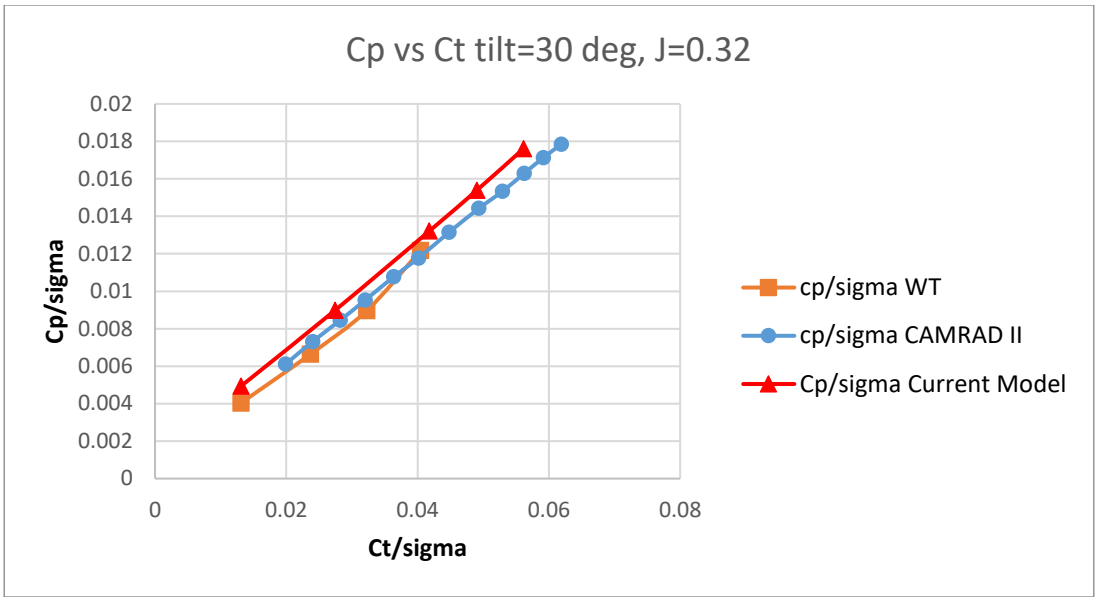

Figure 22: Comparison of C_P vs C_T for Wind tunnel (WT), CAMRAD II and current model data at advance ratio of 0.32 and nacelle angle of 30 degrees.

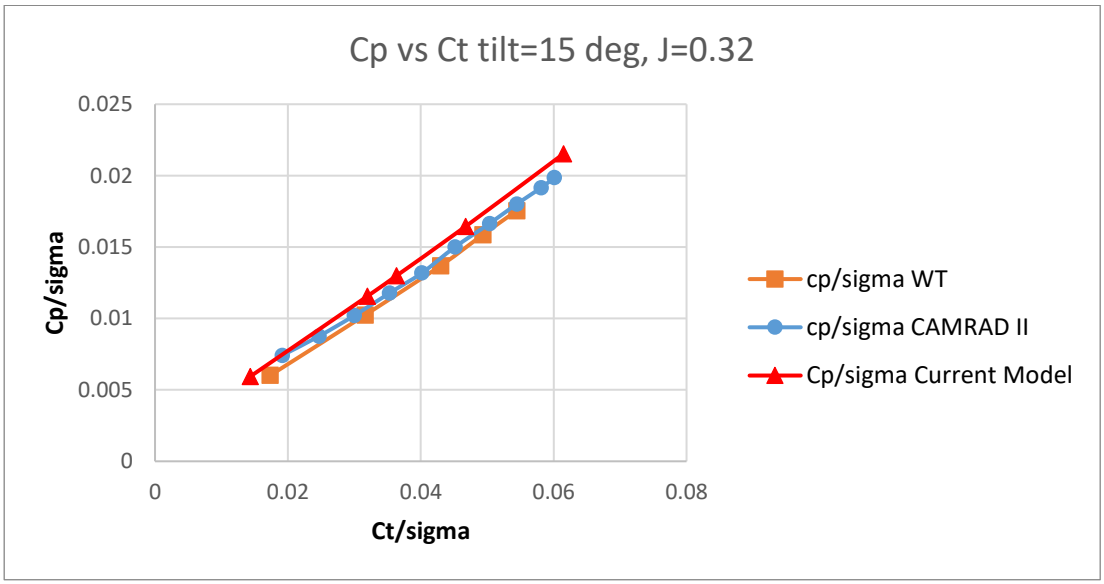

Figure 23: Comparison of C_P vs C_T for Wind tunnel (WT), CAMRAD II and current model data at advance ratio of 0.32 and nacelle angle of 15 degrees.

References

The History of the XV-15 Tilt Rotor Research Aircraft from Concept to Flight
Empirical Modeling of Tilt-Rotor Aerodynamic Performance Empirical Modeling of Tilt-Rotor Aerodynamic Performance
An Assessment of Capability To Calc Tilting Prop-Rotor Aircraft Performance, Loads, and Stability
Modeling and Analysis of Tilt-Rotor Aeromechanical Phenomena
Prop-rotor design for an electric tilt-rotor vehicle

[1]
Drela M., "XROTOR, Ver. 7.69: An interactive program for design and analysis of ducted and free-tip propellers and windmills," https://web.mit.edu/drela/Public/web/xrotor. Accessed May 2022.
[2] Johnson W., "An assessment of the Capability to Calculate Tilting Prop-rotor Aircraft Performance, Loads, and Stability," NASA TP 2291, pp. 1-21, 1984.
[3] Koning W. J.F., "Wind Tunnel Interference Effects on Tiltrotor Testing using Computational Fluid Dynamics", NASA/CR-2016-219086, March 2016
[4] Maisel M., Giulanetti D.J., Dugan D.C., "The History of XV-15 Tilt Rotor Research Aircraft from Concept to Flight", NASA SP-2000-4517
[5] Johnson W., "CAMRAD II Comprehensive Analytical Model of Rotorcraft Aerodynamics and Dynamics", Johnson Aeronautics, Palo Alto, CA, 2005